Preprint submitted to
SAMPLING THEORY IN SIGNAL AND IMAGE PROCESSING

DVI file produced on

Shearlets as Multi-scale Radon Transforms

Francesca Bartolucci
DIMA, Università di Genova, Via Dodecaneso 35
Genova, 16146, Italy
bartolucci@dima.unige.it
Filippo De Mari
DIMA, Università di Genova, Via Dodecaneso 35
Genova, 16146, Italy
demari@dima.unige.it
Ernesto De Vito
DIMA, Università di Genova, Via Dodecaneso 35
Genova, 16146, Italy
devito@dima.unige.it
Francesca Odone
DIBRIS, Università di Genova, Via Dodecaneso 35
Genova, 16146, Italy
francesca.odone@unige.it

Abstract. We show that the 2D-shearlet transform is the composition of the affine Radon transform, a 1D-wavelet transform and a 1D-convolution.

Key words and phrases : Shearlets, Wavelets, Radon Transform

2010 AMS Mathematics Subject Classification — 42C40

1. Introduction

Many effective algorithms in signal analysis, image processing and computer vision are based on efficient multi-scale representations. It is well known that wavelets provide an almost optimal framework for 1D-signals, whereas for multi-dimensional signals a huge class of representations has been introduced like directional wavelets [1], ridgelets [4], curvelets [5], wavelets with composite dilations [19], contourlets [11], shearlets [26], reproducing groups of the symplectic group [16], Gabor ridge functions [16] and mocklets [9] – to name a few.

Among them, shearlets emerge because of their ability to efficiently capture anisotropic features, to provide an optimal sparse representation, to detect singularities and to be stable against noise. The effectiveness of shearlets is supported by the well-established mathematical theory of square-integrable representations and it is tested in many applications in image processing, where many efficient algorithms based on shearlets have been designed (see [24, 12] and also the website `http://www.shearlab.org/` for further details and references).

For these reasons, it is natural to observe that shearlets for 2D-signals behave as wavelets for 1D-signals, so that one could try to understand if this strong connection is a consequence of some general mathematical principle.

In the papers [3], [2] it is shown that the Radon transform is the link between the shearlet transform and the 1D-wavelet transform since it intertwines the shearlet representation with a suitable tensor product of two wavelet representations. Based on the properties of the Radon transform and the 1D-wavelet transform, in this paper we provide an alternative proof that the shearlet transform is able to resolve the wavefront set associated with the unit disc. Classical proofs are given in [23], [17], [25].

The role of the Radon transform in signal analysis is an issue that has already been addressed. Indeed it is known that ridgelets are constructed via wavelet analysis in the Radon domain [13], Gabor frames are defined as the directionally-sensitive Radon transforms [16], discrete shearlet frames are used to invert the Radon transform [6] and the Radon transform is at the root of the proof that shearlets are able to detect the wavefront set of a 2D-signal [17]. Our contribution in this circle of ideas is to clarify this relation from the point of view of non-commutative harmonic analysis.

The paper is organised as it follows. In Section 2 we briefly recall the wavelet, shearlet and Radon transforms. In Section 3 we state the main results, and in Section 4 we show further results for d-dimensional signals. Section 5 contains a sketch of the proofs and Section 6 shows how our results can be used in the problem of characterising the wavefront set of a signal. Finally, Section 7 is left to some concluding remarks.

2. **Wavelet, shearlet and Radon transforms: an overview**

We briefly introduce the notation. We set $\mathbb{R}^* = \mathbb{R}\backslash\{0\}$, regarded as multiplicative group. The scalar product and the norm of $\mathbb{R}^d$ are denoted by $\vec{n}\cdot\vec{n}'$ and $|\vec{n}|$, respectively. We denote by $L^p(\mathbb{R}^d)$ the Banach space of functions $f : \mathbb{R}^d \to \mathbb{C}$, which are p-integrable with respect to the Lebesgue measure $d\vec{x}$ and, if $p = 2$, the corresponding scalar product and norm are $\langle f, g\rangle$ and $\|f\|$. The Fourier transform is denoted by $\mathcal{F}$ both on $L^2(\mathbb{R}^d)$ and on $L^1(\mathbb{R}^d)$, where it is defined by

$$\mathcal{F}f(\vec{\xi}) = \int_{\mathbb{R}^d} f(x,y)\mathrm{e}^{-2\pi i\,\vec{\xi}\cdot\vec{x}}\mathrm{d}\vec{x}, \qquad f \in L^1(\mathbb{R}^d).$$

If G is a locally compact group, $L^2(G)$ is the Hilbert space of square-integrable functions with respect to a left Haar measure.

2.1. **Wavelets.**

The wavelet group is $\mathbb{W} = \mathbb{R} \rtimes \mathbb{R}^*$ with group law

$$(b, a)(b', a') = (b + ab', aa').$$

The wavelet representation W acts on $L^2(\mathbb{R})$ as

$$W_{b,a}\psi(x) = |a|^{-1/2}\psi(\frac{x-b}{a}), \qquad x \in \mathbb{R},$$

and the wavelet transform $\mathcal{W}_\psi : L^2(\mathbb{R}) \to L^2(\mathbb{W})$

$$\mathcal{W}_\psi f(b,a) = \langle f, W_{b,a}\psi \rangle, \quad (b,a) \in \mathbb{W}$$

is a (non-zero) multiple of an isometry provided that

$$0 < \int_{\mathbb{R}} \frac{|\mathcal{F}\psi(\xi)|^2}{|\xi|}\, \mathrm{d}\xi < +\infty.$$

In this case, ψ is called an admissible wavelet [14, 10].

2.2. **Shearlets.** Given $\gamma \in \mathbb{R}$, the shearlet group is $\mathbb{S}^\gamma = \mathbb{R}^2 \rtimes (\mathbb{R} \rtimes \mathbb{R}^*)$ with group law

$$(\vec{b}, s, a)(\vec{b}', s', a') = (\vec{b} + N_s A_a \vec{b}', s + |a|^{1-\gamma} s', aa')$$

where

$$A_a = a \begin{bmatrix} 1 & 0 \\ 0 & |a|^{\gamma-1} \end{bmatrix} \quad N_s = \begin{bmatrix} 1 & -s \\ 0 & 1 \end{bmatrix}$$

and the vectors are understood as column vectors. Parabolic shearlets, which were introduced in [26], correspond to the choice $\gamma = 1/2$. The group $\mathbb{S}^\gamma$ acts on $L^2(\mathbb{R}^2)$ as

$$S^\gamma_{\vec{b},s,a} f\,(\vec{x}) = |a|^{-\frac{1+\gamma}{2}} f(A_a^{-1} N_s^{-1}(\vec{x} - \vec{b})), \qquad \vec{x} \in \mathbb{R}^2,$$

and the shearlet transform $\mathcal{S}^\gamma_\psi : L^2(\mathbb{R}^2) \to L^2(\mathbb{S}^\gamma)$

$$\mathcal{S}^\gamma_\psi f(\vec{b}, s, a) = \langle f, S^\gamma_{\vec{b},s,a}\psi \rangle, \qquad (\vec{b}, s, a) \in \mathbb{S}^\gamma$$

is a (non-zero) multiple of an isometry provided that

$$0 < \int_{\mathbb{R}^2} \frac{|\mathcal{F}\psi(\xi_1,\xi_2)|^2}{|\xi_1|^2} \mathrm{d}\xi_1 \mathrm{d}\xi_2 < +\infty. \tag{1}$$

Classical mother shearlets [26] are of the form

$$\mathcal{F}\psi(\xi_1,\xi_2) = \mathcal{F}\psi_1(\xi_1)\mathcal{F}\psi_2\left(\frac{\xi_2}{\xi_1}\right),$$

where ψ_1 is an admissible wavelet and $\mathcal{F}\psi_2$ is a bump function in the Fourier domain [7]. An example of shearlet ψ is depicted in Fig. 1. In [22] a different choice for the mother wavelets has been proposed to have compactly supported shearlets in the space domain.

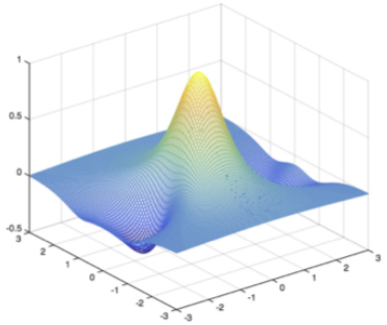

Figure 1. A *classical* mother shearlet ψ in the space domain.

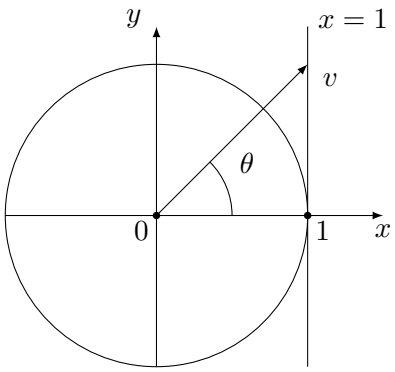

Figure 2. The affine coordinates.

2.3. **Radon transforms.** The Radon transform [20] is usually defined by labeling the lines by pairs $(\theta, q) \in [-\pi, \pi) \times \mathbb{R}$, that is

$$\Gamma_{\theta,q} = \{(x, y) \in \mathbb{R}^2 \mid x \cos\theta + y \sin\theta = q\}.$$

To stress the dependency on the polar angle θ we write

$$\mathcal{R}^{\mathrm{pol}} f(\theta, q) = \int\limits_{x\cos\theta + y\sin\theta = q} f(x, y)\, \mathrm{d}\ell(x, y),$$

where $\mathrm{d}\ell$ is the measure on the line $\Gamma_{\theta,q}$. We label the normal vector to a line by affine coordinates, see Fig. 2, writing

$$\Gamma_{v,t} = \{(x, y) \in \mathbb{R}^2 \mid x + vy = t\}$$

where the correspondence is $v = \tan\theta$ and $t = q/\cos\theta$. With this parametrisation, the vertical lines, which correspond to the choice $\theta = \pm\pi/2$, can not be represented, but they constitute a negligible set with respect to the natural measure on the affine projective space $\mathbb{P}^1 \times \mathbb{R} = \{\Gamma \mid \Gamma \text{ line of } \mathbb{R}^2\}$.

The (affine) Radon transform of any $f \in L^1(\mathbb{R}^2)$ is the function $\mathcal{R}f : \mathbb{R}^2 \to \mathbb{C}$ defined by

$$\mathcal{R}f(v,t) = \int_{\mathbb{R}} f(t - vy, y)\,\mathrm{d}y, \qquad \text{a.e. } (v,t) \in \mathbb{R}^2$$

and is related to the (polar) Radon transform by

$$\mathcal{R}f(v,t) = \frac{1}{\sqrt{1+v^2}}\mathcal{R}^{\mathrm{pol}}f(\arctan v, \frac{t}{\sqrt{1+v^2}}). \tag{2}$$

The central Fourier slice theorem [20] shows that the Radon transform is strongly related to the Fourier transform since for any $f \in L^1(\mathbb{R}^2)$ it holds that

$$(I \otimes \mathcal{F})\mathcal{R}f(v,\omega) = \mathcal{F}f(\omega, \omega v) \qquad (v,\omega) \in \mathbb{R}^2. \tag{3}$$

As in the case of the Fourier transform, it is possible to extend $\mathcal{R}$ to $L^2(\mathbb{R}^2)$ as a unitary map. However, this raises some technical issues. First, consider the subspace

$$\mathcal{D} = \{g \in L^2(\mathbb{R}^2) \mid \int_{\mathbb{R}^2} |\omega||(I \otimes \mathcal{F})g(v,\omega)|^2 \mathrm{d}v\mathrm{d}\omega < +\infty\},$$

which is a dense subset of $L^2(\mathbb{R}^2)$, and then define the self-adjoint unbounded operator $\mathcal{J} : \mathcal{D} \to L^2(\mathbb{R}^2)$ by

$$(I \otimes \mathcal{F})\mathcal{J}F(v,\omega) = |\omega|^{\frac{1}{2}}(I \otimes \mathcal{F})F(v,\omega), \qquad \text{a.e. } (v,\omega) \in \mathbb{R}^2,$$

which is a Fourier multiplier with respect to the second variable. Then, it is not hard to show that for all f in the dense subspace of $L^2(\mathbb{R}^2)$

$$\mathcal{A} = \{f \in L^1(\mathbb{R}^2) \cap L^2(\mathbb{R}^2) \mid \int_{\mathbb{R}^2} \frac{|\mathcal{F}f(\xi_1,\xi_2)|^2}{|\xi_1|}\mathrm{d}\xi_1\mathrm{d}\xi_2 < +\infty\},$$

the Radon transform $\mathcal{R}f$ belongs to $\mathcal{D}$ and the map

$$f \longmapsto \mathcal{J}\mathcal{R}f$$

from $\mathcal{A}$ to $L^2(\mathbb{R}^2)$ extends to a unitary map, denoted by $\mathcal{Q}$, from $L^2(\mathbb{R}^2)$ onto itself. We need the following generalisation of the Fourier slice theorem.

Corollary 1 ([3], [2])**.** *For all $f \in L^2(\mathbb{R}^2)$*

$$(I \otimes \mathcal{F})\mathcal{Q}f(v,\omega) = |\omega|^{\frac{1}{2}}\mathcal{F}f(\omega,\omega v), \qquad \textit{a.e. } (v,\omega) \in \mathbb{R}^2. \tag{4}$$

If $f \in \mathcal{A}$, (4) is an easy consequence of (3) and the definition of $\mathcal{J}$, and this is known (see [6], Section 3.2 and [28]). For arbitrary $f \in L^2(\mathbb{R}^2)$ the proof is not trivial because $\mathcal{Q}$ cannot be written as $\mathcal{J}\mathcal{R}$, and is based on the fact that $\mathcal{J}$ is a Fourier multiplier.

3. Main results

The next result shows that $\mathcal{Q}$ intertwines the shearlet representation S^γ with the tensor product of two wavelet representations W.

Theorem 2 ([3], [2]). *For all $(\vec{b}, s, a) \in \mathbb{S}^\gamma$ and $f \in L^2(\mathbb{R}^2)$*

$$\mathcal{Q}\, S^\gamma_{\vec{b},s,a} f = \left(W_{s,|a|^{1-\gamma}} \otimes \mathrm{I}\right) W_{(1,\bullet)\cdot\vec{b},a}\, \mathcal{Q} f. \tag{5}$$

In (5) the action of the operator $W_{(1,\bullet)\cdot\vec{b},a}$ on a function $F \in L^2(\mathbb{R}^2)$ is

$$W_{(1,\bullet)\cdot\vec{b},a} F(v,t) = |a|^{-\frac{1}{2}} F\left(v, \frac{t - (1,v)\cdot\vec{b}}{a}\right).$$

For a sketch of the proof of Theorem 2 see Section 5. We next discuss under which conditions on the analyzing functions it is possible to write an applicable formula for the shearlet coefficients, such as formula (8) below. Eq. (5) suggests that a natural choice for the admissible vector ψ is of the form

$$\mathcal{Q}\psi = \phi_2 \otimes \phi_1$$

where $\phi_1, \phi_2 \in L^2(\mathbb{R})$. As a consequence of (4),

$$\mathcal{F}\psi(\xi_1,\xi_2) = \mathcal{F}\psi_1(\xi_1)\mathcal{F}\psi_2(\frac{\xi_2}{\xi_1})$$

where

$$\mathcal{F}\phi_1(\omega) = |\omega|^{\frac{1}{2}}\mathcal{F}\psi_1(\omega), \qquad \phi_2(v) = \mathcal{F}\psi_2(v).$$

The admissibility condition (1) is equivalent to requiring that ψ_1 satisfies

$$0 < \int_{\mathbb{R}} \frac{|\mathcal{F}\psi_1(\omega)|^2}{|\omega|} \mathrm{d}\omega < +\infty,$$

$$\int_{\mathbb{R}} |\omega| |\mathcal{F}\psi_1(\omega)|^2 \mathrm{d}\omega < +\infty$$

and ψ_2 is a nonzero function in $L^2(\mathbb{R})$. This means that ψ_1 is a 1D-wavelet in the (fractional) Sobolev space $H^{\frac{1}{2}}(\mathbb{R})$. Furthermore, it is possible to prove that ϕ_1 is an admissible wavelet, too, and that

$$\mathcal{S}^\gamma_\psi(f)(x,y,s,a) = |a|^{\frac{\gamma-1}{2}} \int_{\mathbb{R}} \mathcal{W}_{\phi_1}\big(\mathcal{Q}f(v,\bullet)\big)(x+vy,a)\overline{\phi_2\left(\frac{v-s}{|a|^{1-\gamma}}\right)}\,\mathrm{d}v, \tag{6}$$

where $\mathcal{W}_{\phi_1}\big(\mathcal{Q}f(v,\bullet)\big)$ means that the wavelet transform is computed with respect to the second variable. If ϕ_2 is a bump function, the behaviour of the integral (6) depends on the value of γ. Indeed, if a goes to zero and $\gamma < 1$, $\phi_2\left(\frac{v-s}{|a|^{1-\gamma}}\right)$ is an approximation of the identity, whereas if $\gamma > 1$, it looks like a scale dependent smoothing. In signal analysis usually $\gamma = 1/2$.

Eq. (6) is not easy to implement in applications since the definition of $\mathcal{Q}$ involves both a limit and the pseudo differential operator $\mathcal{J}$. However, if $\phi_2 \otimes \phi_1$ is in the domain of $\mathcal{J}$, we can set $\phi_2 \otimes \chi_1 = \mathcal{J}(\phi_2 \otimes \phi_1)$, *i.e.*

$$\mathcal{F}\chi_1(\omega) = |\omega| \mathcal{F}\psi_1(\omega), \tag{7}$$

so that $\chi_1 = \frac{1}{2\pi} \mathrm{H}\, \psi_1'$, where $'$ is the weak derivative and H is the Hilbert transform. With this choice, χ_1 is an admissible wavelet, too, and it holds that

$$\mathcal{S}_\psi^\gamma f(x,y,s,a) = |a|^{\frac{\gamma-2}{2}} \int_{\mathbb{R}} \mathcal{W}_{\chi_1}\big(\mathcal{R}f(v,\bullet)\big)(x+vy,a) \overline{\phi_2\Big(\frac{v-s}{|a|^{1-\gamma}}\Big)}\, \mathrm{d}v \tag{8}$$

for all $f \in \mathcal{A}$. The above formula can be written in terms of the polar Radon transform using (2) and can actually be extended to $L^1(\mathbb{R}^2) \cap L^2(\mathbb{R}^2)$ (see [3]).

Eq. (8) shows that for any signal f in $L^1(\mathbb{R}^2) \cap L^2(\mathbb{R}^2)$ the shearlet coefficients can be computed by means of the following three *classical* transforms:

a) compute the Radon transform $\mathcal{R}f(v,t)$;
b) apply the wavelet transform with respect to the variable t

$$G(v,\vec{b},a) = \mathcal{W}_{\chi_1}\big(\mathcal{R}f(v,\cdot)\big)(\vec{b},a), \tag{9}$$

where χ_1 is given by (7);
c) convolve the result with the scale-dependent filter

$$\Phi_a(v) = \overline{\phi_2\left(-\frac{v}{|a|^{1-\gamma}}\right)},$$

where the convolution is computed with respect to the variable v,

$$\mathcal{S}_\psi^\gamma f(x,y,s,a) = \big(G(\bullet, x+\bullet\, y, a) * \Phi_a\big)(s). \tag{10}$$

Finally, since $\mathbb{S}^\gamma$ is a square-integrable representation, there is a reconstruction formula. Indeed

$$f = \int_{\mathbb{S}^\gamma} \mathcal{S}_\psi^\gamma f(x,y,s,a)\ S_{x,y,s,a}^\gamma \psi\ \frac{\mathrm{d}x\mathrm{d}y\mathrm{d}s\mathrm{d}a}{|a|^3},$$

where the integral converges in the weak sense. Note that $\mathcal{S}_\psi^\gamma f(x,y,s,a)$ depends on f only through its Radon transform $\mathcal{R}f$ (see (9) and (10)). The above equation allows to reconstruct an unknown signal f from its Radon transform by computing the shearlet coefficients by means of (8).

4. **Further extensions**

The construction can be extended to the generalised shearlet groups introduced in [15]. This class of groups consists of semi-direct products $G = \mathbb{R}^d \rtimes H$. The homogenous group H is a closed subgroup of $\mathrm{GL}(d,\mathbb{R})$ of the form

$$H = \{a \begin{bmatrix} 1 & -{}^t\vec{s}\,\Lambda(a) \\ 0 & B(\vec{s})\,\Lambda(a) \end{bmatrix} = h_{\vec{s},a} \mid a \in \mathbb{R}^*, \vec{s} \in \mathbb{R}^{d-1}\},$$

where $\Lambda(a)$ is a diagonal matrix of size $d-1$

$$\begin{bmatrix} |a|^{\lambda_1} & 0 & \dots & 0 \\ 0 & |a|^{\lambda_2} & \dots & 0 \\ 0 & \dots & \ddots & 0 \\ 0 & \dots & \dots & |a|^{\lambda_{d-1}} \end{bmatrix}$$

and $B(\vec{s})$ is a unipotent upper triangular matrix of size $d-1$

$$B(\vec{s}) = \begin{bmatrix} 1 & * & \dots & * \\ 0 & 1 & \dots & * \\ 0 & \dots & \ddots & * \\ 0 & \dots & \dots & 1 \end{bmatrix}.$$

For example, the shearlet group for d-dimensional signals introduced in [8] corresponds to the choices $B(\vec{s}) = \mathrm{I}_{d-1}$ and $\lambda_1 = \ldots = \lambda_{d-1} = 1/d - 1$. If $d = 2$ we get the shearlet group introduced in Section 2.

Remark 1. The group H is the semi-direct product of the normal subgroup

$$S = \{ \begin{bmatrix} 1 & -{}^t\vec{s} \\ 0 & B(\vec{s}) \end{bmatrix} \mid \vec{s} \in \mathbb{R}^{d-1} \}$$

and the abelian subgroup

$$D = \{ a \begin{bmatrix} 1 & 0 \\ 0 & \Lambda(a) \end{bmatrix} \mid a \in \mathbb{R}^* \}.$$

Clearly, D is isomorphic, as a Lie group, to $\mathbb{R}^*$. For classical shearlets, S is isomorphic as a Lie group to the additive abelian group $\mathbb{R}^{d-1}$. In the general setting, S is diffeomorphic to $\mathbb{R}^{d-1}$ only as a manifold. In order to stress the symmetry between the general case and the classical shearlet group, we identify H and $\mathbb{R}^{d-1} \times \mathbb{R}^*$ as a manifold and we denote the element $h_{\vec{s},a}$ with the pair $(\vec{s}, a)$. We observe that $(\vec{s}, a) = (\vec{s}, 1)(\vec{0}, a)$ since $h_{\vec{s},a} = h_{\vec{s},1} h_{0,a}$, however in general

$$(\vec{s}, 1)(\vec{s}\,', 1) \neq (\vec{s} + \vec{s}\,', 1).$$

The map $\vec{s} \mapsto B(\vec{s})$ has to satisfy natural algebraic conditions to ensure that S is a subgroup of $\mathrm{GL}(d, \mathbb{R})$. Furthermore, suitable compatibility conditions between the matrices B and the matrices Λ must be satisfied. A complete characterisation of the maps $B(\cdot)$ and $\Lambda(\cdot)$ is given in [15] under the assumption that S is abelian.

The group G acts on $L^2(\mathbb{R}^d)$ as

$$\pi_{\vec{b},\vec{s},a} f(\vec{x}) = |a|^{-\frac{d+\lambda_1+\ldots+\lambda_{d-1}}{2}} f(h^{-1}_{\vec{s},a}(\vec{x} - \vec{b})).$$

Eq. (5) is replaced by

$$\mathcal{Q}\, \pi_{\vec{b},\vec{s},a} f = \left(V_{\vec{s},a} \otimes \mathrm{I}\right) W_{(1,\mathbf{v})\cdot\vec{b},a}\, \mathcal{Q} f,$$

where V is the representation of H on $L^2(\mathbb{R}^{d-1})$ defined by

$$V_{\vec{s},a}F(\vec{v}) = |a|^{\frac{\lambda_1+\ldots+\lambda_{d-1}}{2}} F\left(\Lambda(a)\left({}^tB(\vec{s})\vec{v} - \vec{s}\right)\right).$$

5. **Sketch of the proof**

We give an idea of the proof of Theorem 2. By continuity it is enough to show (5) assuming that $f \in \mathcal{A}$, so that $\mathcal{Q} = \mathcal{J}\mathcal{R}$.

The following covariance properties of the Radon transform are an easy consequence of the appropriate changes of variables. For any translation $\vec{b} \in \mathbb{R}^2$ it holds

$$\mathcal{R}\left(f(\cdot - \vec{b})\right)(v,t) = \mathcal{R}[f](v, t - (1,v)\cdot\vec{b});$$

for any invertible diagonal matrix

$$A = \begin{bmatrix} a_1 & 0 \\ 0 & a_2 \end{bmatrix}, \qquad a_1, a_2 \in \mathbb{R}^* \tag{11}$$

it holds

$$\mathcal{R}\left(f(A^{-1}\cdot)\right)(v,t) = |a_2|\,\mathcal{R}f(\frac{a_2}{a_1}v, a_1 t),$$

and for any shearing matrix

$$N = \begin{bmatrix} 1 & -s \\ 0 & 1 \end{bmatrix}, \qquad s \in \mathbb{R}$$

it holds

$$\mathcal{R}\left(f(N^{-1}\cdot)\right)(v,t) = \mathcal{R}[f](v - s, t).$$

Moreover the operator $\mathcal{J}$ clearly commutes with translations and shearings, whereas, if A is as in (11),

$$\mathcal{J}\left(F(A^{-1}\cdot)\right)(v,\omega) = |a_2|^{\frac{1}{2}}\mathcal{J}F(a_1^{-1}v, a_2\omega).$$

The final step is to observe that, if $f \in \mathcal{A}$, then

$$\mathcal{Q}\,S^{\gamma}_{\vec{b},s,a}f = \mathcal{J}\mathcal{R}S^{\gamma}_{\vec{b},0,1}S^{\gamma}_{0,s,1}S^{\gamma}_{0,0,a}f$$

and apply three times the above covariance relations.

6. **Wavefront set resolution**

Among the huge class of directional multiscale representations, shearlets have gained considerable attention for their capability to resolve the wavefront set of distributions, providing both the location and the geometry of the singularity set. In [23] the authors show that the decay rate of the shearlet coefficients of a temperate distribution f with respect to suitable shearlets characterises the wavefront set of f. Later this result has been generalised in [17], in which it is shown that the same result can be verified under much weaker assumptions on the continuous shearlets by means of a new approach based on the affine Radon transform. Further results in this line of research are given in [18, 25, 21]. In this section we show that our result can provide some geometric insight on the ability of the shearlet transform to resolve the wavefront set.

We recall that, given a distribution f, a point $\vec{x} \in \mathbb{R}^2$ is a regular point of f, if there exists a function $\phi \in C_0^\infty(U_{\vec{x}})$, where $U_{\vec{x}}$ is a neighborhood of $\vec{x}$ and $\phi(\vec{x}) \neq 0$, such that $\phi f \in C_0^\infty(\mathbb{R}^2)$, which is equivalent to $\mathcal{F}(\phi f)$ being rapidly decreasing. The complement of the set of regular points of f is called the singular support of f. Furthermore a point $(\vec{x}, \vec{n}) \in \mathbb{R}^2 \times \mathbb{R}^2$, $\vec{n} \neq 0$ is a regular directed point, if there exist a neighborhood $U_{\vec{x}}$ of $\vec{x}$ and a conic neighborhood $V_{\vec{n}}$ of $\vec{n}$ as well as a function $\phi \in C_0^\infty(\mathbb{R}^2)$ satisfying $\phi_{|_{U_{\vec{x}}}} \equiv 1$ such that, for each $N > 0$, there exists a constant C_N with

$$|\mathcal{F}(\phi f)(\vec{\xi})| \leq C_N (1 + |\vec{\xi}|)^{-N} \tag{12}$$

for all $\vec{\xi} \in \mathbb{R}^2$ such that $\vec{\xi} \in V_{\vec{n}}$. The complement of the regular directed points of f is called the wavefront set of f and is denoted by $WF(f)$. It is worth observing that the projection $WF(f) \ni (\vec{x}, \vec{n}) \mapsto \vec{x} \in \mathbb{R}^2$ gives the singular support of f. Therefore, through the notion of wavefront set we describe not only where the singular support of f is located but also how it is distributed.

Formula (8) gives an alternative way to show that the shearlet transform is able to resolve the wavefront set of distributions. Our approach is based on geometric observations and on the fact that the Fourier slice theorem (3) indicates that the Radon transform is a useful tool in microlocal analysis. To give an idea of how it works, we present the example of the characteristic function of the unit disc, namely

$$f(x,y) = \begin{cases} \frac{1}{2} & x^2 + y^2 \leq 1 \\ 0 & x^2 + y^2 > 1 \end{cases},$$

depicted in Fig. 3 (the factor $1/2$ is introduced to simplify subsequent computations).

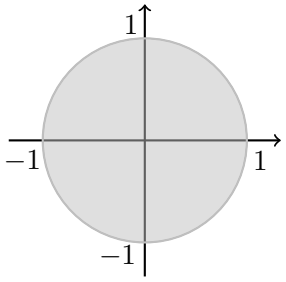

Figure 3. Characteristic function on the unit disc.

A simple calculation shows that the wavefront set of f is

$$WF(f) = \{\big(\cos\theta, \sin\theta, \lambda\cos\theta, \lambda\sin\theta\big) \mid \theta \in (-\pi, \pi],\ \lambda \in \mathbb{R}^*\}. \tag{13}$$

The affine Radon transform of f is

$$\mathcal{R}f(v,t) = \begin{cases} \frac{\sqrt{1+v^2-t^2}}{1+v^2} & t^2 - v^2 \leq 1 \\ 0 & t^2 - v^2 > 1. \end{cases} \tag{14}$$

As a consequence of the rotational invariance of f, it holds that

$$\mathcal{R}f(v,t) = \frac{1}{\sqrt[4]{1+v^2}}(W_{0,\sqrt{1+v^2}}\varphi)(t), \tag{15}$$

where

$$\varphi(t) = \begin{cases} \sqrt{1-t^2} & |t| \leq 1 \\ 0 & |t| > 1 \end{cases},$$

which is depicted in Fig. 4.

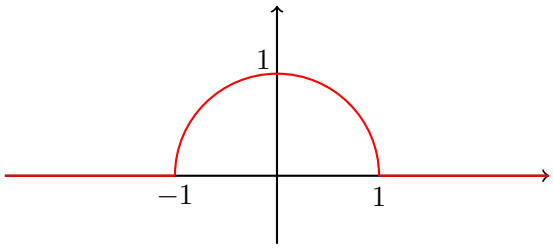

Figure 4. $\mathcal{R}f(0,t) = \varphi(t)$.

By formula (8) and (15) and by the fact that the wavelet transform commutes with dilations, we obtain

$$\mathcal{W}_{\chi_1}\big(\mathcal{R}f(v,\bullet)\big)(b,a) = \frac{1}{\sqrt[4]{1+v^2}}(\mathcal{W}_{\chi_1}\varphi)\,(\frac{b}{\sqrt{1+v^2}}, \frac{a}{\sqrt{1+v^2}}). \tag{16}$$

The wavelet transform of φ is depicted in Fig. 5

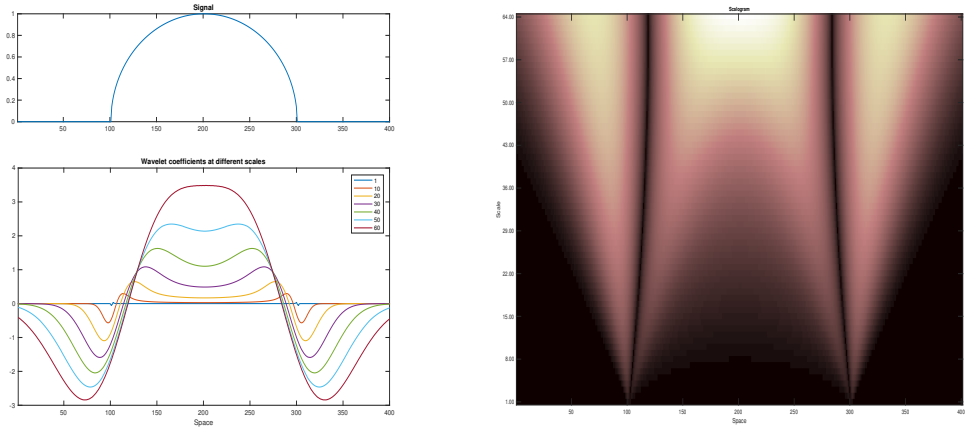

Figure 5. The wavelet coefficients at different scales.

and, as expected, the wavelet coefficients $\mathcal{W}_{\chi_1}\varphi(b,a)$ of φ slowly decrease if and only if $b = \pm 1$ when a goes to zero. Recall that, if χ_1 has compact support

equal to $[-1,1]$, the singularities in $t = \pm 1$ create cones of influence in the scale-space plane defined by

$$|b \mp 1| \leq a,$$

to which the high amplitude wavelet coefficients belong, i.e. the wavelet coefficients which do not exhibit rapid asymptotic decay at $b = \pm 1$, as $a \to 0$. The cones of influence created by the singular points $t = \pm 1$ are clearly visible in Fig. 5 (see Chapter 6 in [27] for further details). We now show that this behaviour implies the ability of the shearlet transform to correctly detect the wavefront set of the distribution f.

As we did for the Radon transform, we now parametrise the direction $\vec{n}$ by using affine coordinates, so that (13) reads

$$WF(f)_0 = \{(\cos\theta, \sin\theta, \tan\theta) \mid \theta \in (-\pi, \pi], \theta \neq \pm\frac{\pi}{2}\}.$$

Here $WF(f)_0$ is the wavefront set of f whose singular support does not intersect the vertical axis, *i.e.* the points $(0, \pm 1, 0, \lambda)$ and, with slight abuse of notation, each $s \in \mathbb{R}$ denotes the set of directions $\{\vec{n} = \lambda(1, s) \mid \lambda \in \mathbb{R}^*\}$.

We start by considering a point $(\vec{x}, s) \notin WF(f)_0$, *i.e* a regular directed point. So, by definition, there exist neighborhoods $U_{\vec{x}}$ of $\vec{x}$ and V_s of s as well as a function $\phi \in C_0^\infty(\mathbb{R}^2)$ satisfying $\phi_{|U_{\vec{x}}} \equiv 1$ such that (12) is satisfied for any $N > 0$ and for all $\vec{\xi} = (\xi_1, \xi_2) \in \mathbb{R}^2$ with $\xi_2/\xi_1 \in V_s$. We want to prove that the shearlet coefficients $\mathcal{S}_\psi f(x, y, s, a)$ have rapid asymptotic decay, as $a \to 0$, where we have parametrised $\vec{x} = (x, y)$. From now on, we consider only the case $a > 0$, the case $a < 0$ is analogous. We require that the mother shearlet ψ is a rapidly decreasing function, so we can assume, without loss of generality, that f is localised around $\vec{x}$. If we suppose that χ_1 has infinitely many vanishing moments and $\mathcal{F}\chi_1 \in L^1(\mathbb{R})$, by formula (8), we prove that the wavelet coefficients

$$\mathcal{W}_{\chi_1}\big(\mathcal{R}f(v, \bullet)\big)(x + vy, a) \tag{17}$$

have rapid asymptotic decay at fine scales uniformly over V_s and $U_{\vec{x}}$. Since ϕ_2 is a bump function, we can suppose that supp $\phi_2 \subseteq [-1, 1]$ and the integral in (8) reduces to those v such that $v \in [s - a^{1-\gamma}, s + a^{1-\gamma}]$, so that, for $a \to 0$, formula (8) becomes:

$$\mathcal{S}_\psi^\gamma f(x, y, s, a) = a^{\frac{\gamma-2}{2}} \int_{V_s} \mathcal{W}_{\chi_1}\big(\mathcal{R}f(v, \bullet)\big)(x + vy, a)\, \overline{\phi_2\Big(\frac{v - s}{a^{1-\gamma}}\Big)}\, \mathrm{d}v \tag{18}$$

For reasons that will be clear below we suppose $\phi_2(v) = 1$ if $v \in [-1/2, 1/2]$. Therefore, from (18) and (17), we obtain the decay estimate

$$\mathcal{S}_\psi f(x, y, v, a) = O(a^N),\ a \to 0$$

for all $N > 0$, uniformly over V_s and $U_{\vec{x}}$. So, we have proved that for any regular directed point $(\vec{x}, s)$ of f the shearlet coefficients, with respect to any shearlet with building block χ_1 with infinitely many vanishing moments, have rapid asymptotic decay at fine scales uniformly around $\vec{x}$ and s.

Now, take a point in the wavefront set $(\cos\theta_s, \sin\theta_s, s)$, with $s = \tan\theta_s$. From (16), we obtain

$$|\mathcal{S}_\psi f(\cos\theta_s, \sin\theta_s, s, a)| = |a^{\frac{\gamma-2}{2}} \int_{s-a^{1-\gamma}}^{s+a^{1-\gamma}} \mathcal{W}_{\chi_1}\varphi(\cos(\theta_s - \theta_v), \frac{a}{\sqrt{1+v^2}}) \overline{\phi_2\Big(\frac{v-s}{a^{1-\gamma}}\Big)} \frac{\mathrm{d}v}{\sqrt[4]{1+v^2}}|, \tag{19}$$

where $\theta_v = \arctan v$. By the mean value theorem, there is $\overline{v} \in [s-a^{1-\gamma}, s+a^{1-\gamma}]$ such that equation (19) can be continued with the string of inequalities

$$\begin{aligned} 2a^{\frac{\gamma-1}{2}} |\frac{1}{\sqrt[4]{1+\overline{v}^2}} \mathcal{W}_{\chi_1}\varphi(\cos(\theta_s - \theta_{\overline{v}}), \frac{a}{\sqrt{1+\overline{v}^2}}) \overline{\phi_2\left(\frac{\overline{v}-s}{a^{1-\gamma}}\right)}| \geq \\ \geq |\frac{1}{\sqrt[4]{1+\overline{v}^2}} \mathcal{W}_{\chi_1}\varphi(\cos(\theta_s - \theta_{\overline{v}}), \frac{a}{\sqrt{1+\overline{v}^2}}) \overline{\phi_2\left(\frac{\overline{v}-s}{a^{1-\gamma}}\right)}|, \end{aligned} \tag{20}$$

where we assume $\gamma < 1$ and $a \leq 1$. The last assumption is not restrictive since we are interested in the behaviour of (20) when a goes to zero. Observe that $\cos(\theta_s - \theta_{\overline{v}}) \to 1$ as $a \to 0$ and that $t = 1$ belongs to the singular support of φ. For this reason, what we should prove, in order to fall within the cone of influence of the singular point $t = 1$, is that the inequality

$$|\cos(\theta_s - \theta_{\overline{v}}) - 1| \leq \frac{a}{\sqrt{1+\overline{v}^2}} \tag{21}$$

holds when a goes to zero, with $\overline{v} \in [s - a^{1-\gamma}, s + a^{1-\gamma}]$. If $\gamma < \frac{1}{2}$, by analysing the decay rate as $a \to 0$ of the right hand side and the left hand side in (21), we can easily conclude that such inequality is satisfied at fine scales. If $\gamma = 1/2$ the following argument can be used:

$$\begin{aligned} |\cos(\theta_s - \theta_{\overline{v}}) - 1|\sqrt{1+\overline{v}^2} &\leq \frac{1}{2}|\theta_s - \theta_{\overline{v}}|^2\sqrt{1+\overline{v}^2} \\ &\leq \frac{1}{2}|s - \overline{v}|^2\sqrt{\frac{1+\overline{v}^2}{1+s^2}} \\ &\leq |s - \overline{v}|^2 \leq a, \end{aligned}$$

where the second inequality is proved applying the Taylor's formula with the remainder in the Lagrange form to the function $t \mapsto |\arctan s - \arctan t|$ and the third inequality is true when a is in a neighborhood of 0. It is worth observing that with this approach the role of γ shows up clearly. Indeed, in order to have inequality (21), the cone created by the bump function ϕ_2 has to be included in the cone of influence associated with the singularity and the parameter γ precisely controls the amplitude of the first cone. Finally, if $1/2 < \gamma < 1$, the situation is still unclear.

This example shows that the ability of the shearlet transform to resolve the wavefront set is a direct consequence of the fact that the wavelet transform is able to describe smoothness of univariate functions. This is seen via formula (8), in which the Radon transform plays a crucial role.

This kind of arguments can be generalised to arbitrary distributions since it is known that there is a geometric construction that relates $WF(\mathcal{R}f)$ and $WF(f)$, based on the Legendre transform (see [29] and also the online lectures `https://www.icts.res.in/sites/default/files/Jan_Boman_Lecture_Notes_0.pdf`).

It is an ongoing project to obtain a new proof of the resolution of the wavefront set for general distributions by means of (8).

This could lead to a new approach based on the affine Radon transform to investigate if a directional multiscale representation is able to resolve the wavefront set of distributions in more general cases.

7. Conclusions

In this paper we show that the shearlet transform of a 2D-signal can be realised by applying first the affine Radon transform, then by computing a 1D-wavelet transform and, finally, by performing a 1D-convolution. This result has been extended to higher dimensional shearlet transforms both in the classical case and for generalised shearlet dilation groups [3]. This relation can give rise to a new algorithm to compute the shearlet coefficients based on the efficient codes available both for the Radon and for the wavelet transforms. Furthermore, it opens the possibility to recover a signal from its Radon transform by using the shearlet inversion formula. The application of these findings to image processing tasks is currently under investigation.

References

[1] J.-P. Antoine and R. Murenzi. Two-dimensional directional wavelets and the scale-angle representation. *Signal processing*, 52(3):259–281, 1996.

[2] F. Bartolucci, F. De Mari, E. De Vito, F. Odone. Shearlets as multi-scale Radon transform. *2017 International Conference on Sampling Theory and Applications (SampTA)*, Tallinn, 2017, pp. 625 - 629.

[3] F. Bartolucci, F. De Mari, E. De Vito, and F. Odone. The Radon transform intertwines wavelets and shearlets. *Applied and Computational Harmonic Analysis*, (2018), *https://doi.org/10.1016/j.acha.2017.12.005*.

[4] E. J. Candès and D. L. Donoho. Ridgelets: A key to higher-dimensional intermittency? *Philosophical Transactions of the Royal Society of London A: Mathematical, Physical and Engineering Sciences*, 357(1760):2495–2509, 1999.

[5] E. J. Candès and D. L. Donoho. New tight frames of curvelets and optimal representations of objects with piecewise C^2 singularities. *Communications on pure and applied mathematics*, 57(2):219–266, 2004.

[6] F. Colonna, G. Easley, K. Guo, and D. Labate. Radon transform inversion using the shearlet representation. *Applied and Computational Harmonic Analysis*, 29(2):232–250, 2010.

[7] S. Dahlke, G. Kutyniok, P. Maass, C. Sagiv, H.-G. Stark, and G. Teschke. The uncertainty principle associated with the continuous shearlet transform. *International Journal of Wavelets, Multiresolution and Information Processing*, 6(02):157–181, 2008.

[8] S. Dahlke, G. Steidl, and G. Teschke. The continuous shearlet transform in arbitrary space dimensions. *Journal of Fourier Analysis and Applications*, 16(3):340–364, 2010.

[9] F. De Mari and E. De Vito. Admissible vectors for mock metaplectic representations. *Applied and Computational Harmonic Analysis*, 34(2):163–200, 2013.

[10] F. De Mari and E. De Vito. The use of representations in applied harmonic analysis. In *Harmonic and Applied Analysis*, pages 7–81. Springer, 2015.
[11] M. N. Do and M. Vetterli. The contourlet transform: an efficient directional multiresolution image representation. *IEEE Transactions on image processing*, 14(12):2091–2106, 2005.
[12] M. A. Duval-Poo, F. Odone, and E. De Vito. Edges and corners with shearlets. *IEEE Transactions on Image Processing*, 24(11):3768–3780, 2015.
[13] J. Fadili and J.-L. Starck. Curvelets and ridgelets. In *Encyclopedia of Complexity and Systems Science*, pages 1718–1738. Springer, 2009.
[14] H. Führ. *Abstract harmonic analysis of continuous wavelet transforms*. Springer, 2005.
[15] H. Führ and R. R. Tousi. Simplified vanishing moment criteria for wavelets over general dilation groups, with applications to abelian and shearlet dilation groups. *Applied and Computational Harmonic Analysis*, 2016.
[16] L. Grafakos and C. Sansing. Gabor frames and directional time–frequency analysis. *Applied and Computational Harmonic Analysis*, 25(1):47–67, 2008.
[17] P. Grohs. Continuous shearlet frames and resolution of the wavefront set. *Monatshefte für Mathematik*, 164(4):393–426, 2011.
[18] K. Guo and D. Labate. Optimally sparse representations of 3D data with C^2 surface singularities using Parseval frames of shearlets. *SIAM J. Math. Anal.*, pages 851–886, 2012.
[19] K. Guo, D. Labate, W.-Q. Lim, G. Weiss, and E. Wilson. Wavelets with composite dilations. *Electronic research announcements of the American Mathematical Society*, 10(9):78–87, 2004.
[20] S. Helgason. *The Radon transform*, volume 5 of *Progress in Mathematics*. Birkhäuser Boston, Inc., Boston, MA, second edition, 1999.
[21] R. Houska and D. Labate. Detection of boundary curves on the piecewise smooth boundary surface of three dimensional solids. *Appl. Comput. Harmon. Anal.*, 40(1):137–171, 2016.
[22] P. Kittipoom, G. Kutyniok, and W.-Q. Lim. Construction of compactly supported shearlet frames. *Constructive Approximation*, 35(1):21–72, 2012.
[23] G. Kutyniok and D. Labate. Resolution of the wavefront set using continuous shearlets. *Trans. Amer. Math. Soc.*, 361(5):2719–2754, 2009.
[24] G. Kutyniok and D. Labate. *Shearlets*. Appl. Numer. Harmon. Anal. Birkhäuser/Springer, New York, 2012.
[25] G. Kutyniok and P. Petersen. Classification of edges using compactly supported shearlets. *Applied and Computational Harmonic Analysis*, 2015.
[26] D. Labate, W.-Q. Lim, G. Kutyniok, and G. Weiss. Sparse multidimensional representation using shearlets. In *Optics & Photonics 2005*, pages 59140U–59140U. International Society for Optics and Photonics, 2005.
[27] S. Mallat. *A wavelet tour of signal processing*. Academic Press, Inc., San Diego, CA, 1998.
[28] F. Natterer. *The mathematics of computerized tomography*. SIAM, 2001.
[29] A. G. Ramm and A. I. Katsevich. *The Radon transform and local tomography*. CRC Press, Boca Raton, FL, 1996.

ACKNOWLEDGEMENT

E. De Vito and F. De Mari are members of the Gruppo Nazionale per l'Analisi Matematica, la Probabilità e le loro Applicazioni (GNAMPA) of the Istituto Nazionale di Alta Matematica (INdAM).